# Modeling of Transport Phenomena in Gas Tungsten Arc Welding of Ni to 304 Stainless Steel

Alireza Bahrami[*1] and Daryush K. Aidun[1]
[1]MAE Department, Clarkson University
*Corresponding author: 8 Clarkson Ave. PO Box 5725 Potsdam, NY 13699, bahrama@clarkson.edu

**Abstract:** This study investigates transport phenomena in the weld pool (WP) of gas tungsten arc (GTA) welding of Nickel to 304 stainless steel. A finite element 3D simulation of fluid flow and heat transfer of spot welding without consumable is accomplished which leads to prediction of the weld zone shape, weld penetration and dilution of alloying elements. The model includes magneto-hydrodynamics (MHD), the effects of surface tension and buoyancy, and the moving interface of solid-liquid.
Different thermophysical properties of alloys subjected to the weld also makes the problem more complicated. Lower melting temperature of 304 as compared to that of Ni leads to creation of an asymmetric WP which is larger in the 304 side. Higher thermal diffusivity of Ni accelerates heat removal in the Ni piece; accordingly maximum temperature happens at the 304 side.

**Keywords:** welding, magneto-hydrodynamics, melting, Marangoni effect, buoyancy force

## 1. Introduction

In the GTA welding process, an arc is established between a non-consumable tungsten electrode and base metals (BM's). An inert shielding gas, such as argon or helium, is introduced to the weld surface to protect the weld from the atmosphere. Besides protection of the weld surface, the shielding gas provides a suitable medium for the initiation of the arc and makes the arc stable. The heat generated by the arc melts the BM's which are consequently joined after solidification [1].

Joining of dissimilar metals/alloys using gas tungsten arc (GTA) welding is extensively used in several industries such as offshore piping and power plants. Thermo-physical, mechanical and metallurgical properties of metals/alloys subjected to dissimilar weld are different; therefore dissimilar welding usually involves complexities [2].

The velocity and temperature fields in dissimilar weld models are asymmetric. As a result, the weld geometry is asymmetric, which necessitates a three dimensional simulation [3].

A 2D axisymmetric model is usually applied in numerical simulations of the spot GTA welding of similar metals [4-8]. In these models electromagnetic force (Lorentz force) and temperature dependent surface tension and density (Marangoni and buoyancy effects) are the driving forces which make the fluid circulate in the WP.

The GTA welding process of 1018 steel to 2205 stainless steel was modeled by the authors [3]. Turbulent convection of molten in laser welding of Cu to Ni was studied by Chakraborty et al [9]. Transport phenomena in dissimilar welding of Fe to Al were simulated numerically by Mukherjee et al [10]. A Ta diffusion barrier was used between the Al and Fe.

The spot GTA welding of Ni to 304 stainless steel is simulated using finite element software COMSOL Multiphysics® 4.3b. The material properties of the solution in the WP are a function of the base metals properties and the mass fraction of the each alloy in the solution of Ni and stainless steel. The simulation results provide the weld geometry and the velocity and temperature fields.

## 2. Mathematical Model

### 2.1 Governing Equations

Figure 1 shows the schematic of the welding model. Coupons of 13mm×26mm×6.35mm of Ni and 304 are placed beside each other. The spot weld is located at the center of the boundary of Ni and 304 coupons.

Following simplifying assumptions have been made, in order to mathematically model the welding process,

- Flow is laminar in the WP;
- A Gaussian distribution of the heat flux and normal current density is applied to simulate the arc;

- Bousinesq approximation is used for the buoyancy convection;
- The mixing of the molten materials in the weld is rapid and uniform;
- The top surface of the melt does not deform.

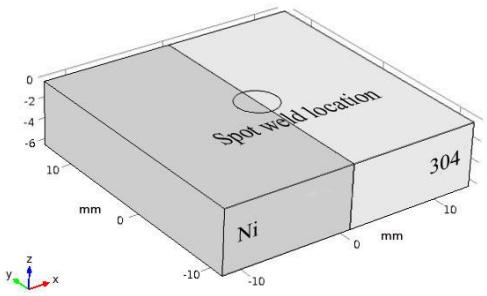


**Figure 1**. Schematic of the geometry of the model

The mass and momentum conservation equations are

$$\frac{\partial \rho}{\partial t} + \nabla.(\rho \mathbf{u}) = 0 \qquad (1)$$

$$\rho \frac{\partial \mathbf{u}}{\partial t} + \rho \mathbf{u}.\nabla \mathbf{u} = \nabla.\left[-p\mathbf{I} + \mu(\nabla \mathbf{u} + (\nabla \mathbf{u})^T) - \frac{2\mu}{3}(\nabla.\mathbf{u})\mathbf{I}\right] + \mathbf{F_d} + \mathbf{F_b} \qquad (2)$$

where ρ and μ denote density and viscosity of the fluid, respectively, $\mathbf{u}$ is the velocity vector and $p$ is the pressure. The source term $\mathbf{F_d}$ is the damping force used to damps the velocity in the solid state. It becomes zero in the liquid phase to let the fluid circulate. This source term is explained in detail in the "Continuous Casting Model" in COMSOL "Model Library".

The other source term in the momentum equation is $\mathbf{F_b}$ which is composed of the volume forces generated by the Lorentz force and gravity driven buoyancy as follows,

$$\mathbf{F_b} = \mathbf{J} \times \mathbf{B} + \rho_0\big(1 - \beta(T - T_s)\big)\mathbf{g} \qquad (3)$$

In this equation $\mathbf{J}$ and $\mathbf{B}$ denote current density and magnetic flux density vectors, respectively. The Maxwell's electromagnetic equations are solved to determine these vectors [11]. $\beta$ is the volume expansion factor and $T_s$ is the solidus temperature.

The energy conservation equation is,

$$\rho C_p' \left(\frac{\partial T}{\partial t} + \mathbf{u}.\nabla T\right) = \nabla.(k\nabla T) \qquad (4)$$

in which $C_p'$ is the apparent heat capacity that take into account the heat of fusion and $k$ is the thermal conductivity coefficient. The apparent heat capacity is defined as

$$C_p' = C_p + \delta(T)\Delta H_f \qquad (5)$$

where $C_p$ and $\Delta H_f$ denote the actual heat capacity and latent heat of fusion, respectively, and $\delta(T)$ is a delta function at the melting temperature.

### 2.2 Boundary Conditions

Gaussian distributions are used for the normal current density and the heat flux from the arc. These distributions are applied to the top surface of the model. The Gaussian distributions of the normal current density and the heat flux are described as [3]

$$j(x,y) = \frac{3I}{\pi a^2} exp\left(\frac{-3(x^2+y^2)}{a^2}\right) \qquad (6)$$

$$q(x,y) = \frac{3Q}{\pi b^2} exp\left(\frac{-3(x^2+y^2)}{b^2}\right) \qquad (7)$$

In these equations $I$ is the arc current and $Q$ is the heat generated by the arc. $a$ and $b$ are the effective radius of the current and heat sources, respectively. The heat of the arc, $Q$ is calculated by the following equation

$$Q = \eta V I \qquad (8)$$

where $\eta$ and $V$ represent the arc efficiency, the arc voltage, respectively.

Surface tension of the molten solution is a function of temperature. The temperature across the surface of the WP varies considerably; accordingly, the change of the surface tension across the surface of the WP is significant. This effect which is called "Marangoni effect" is one of driving forces in the WP. This effect is applied to the model as a boundary condition at the top surface of the WP as [12]

$$\mu \frac{\partial u}{\partial z} = \frac{d\gamma}{dT}\frac{\partial T}{\partial x}$$
$$\mu \frac{\partial v}{\partial z} = \frac{d\gamma}{dT}\frac{\partial T}{\partial y} \qquad (9)$$

$\frac{d\gamma}{dT}$ is the temperature derivative of surface tension.

## 3. Use of COMSOL Multiphysics

Simulation of the GTA welding process includes electromagnetics, fluid flow and heat transfer. Mass transfer also should be studied in the case of dissimilar welding. COMSOL Multiphysics perfectly meets all the requirements of such a complicated simulation.

### 3.1 Multiphysics

In order to calculate the Lorentz force in the WP, "Electric Currents" and "Magnetic Fields" physics where used. Figure 2. shows the domains of the model.The Gaussian distribution of the normal current density is defined in the "Definitions" and applied to the top surfaces of the model in the "Electric Currents" physics. The bottom of the model is grounded. In the "Magnetic Fields" physics an "External Current Density" is added which includes the current density field calculated in the "Electric Currents" physics.

The physics of "Heat Transfer in Fluids" and "Laminar Flow" are employed to simulate the velocity and temperature fields. The "heat transfer" in fluids is applied to the whole model whereas the "laminar flow" is just applied to the part of the model that has the probability of melting (Figure 2).

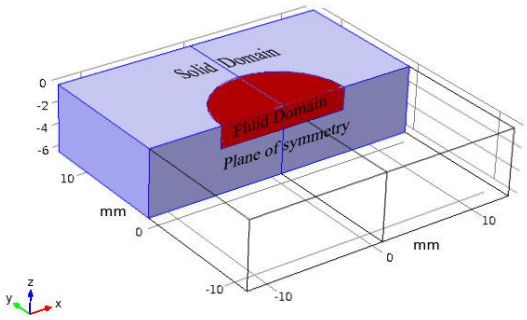


**Figure 2.** Domains of model

To simulate the melting, the "Heat Transfer in Phase Change" node, which is a new ability of 4.3b version, is specified to the tentative liquid domain. The Gaussian distribution of the input heat flux is defined in the definitions and gradually (in 1s) applied to the top surfaces using a step function.

In the "Laminar flow" mode Lorentz force and buoyancy are applied as "Volume Force"s and Marangoni effect is taken into account by employing a "Weak Contribution" at the surface. The detailed explanation is available in the "Marangoni Convection" model in the "Model Library".

### 3.2 Material Properties

One of the most important features of the dissimilar weld simulation is handling the material properties. The material properties in the solid phase are defined as functions of *x* location such that the property changes at *x=0*. The smoothed "Heaviside Function" with a continuous second derivative, "`flc2hs`", is employed to smooth sharp changes of material properties at the boundary of Ni and 304. In the liquid phase it is assumed that the melt mixes rapidly such that the material properties are uniform in the melt. However, the uniform material properties are functions of the properties of the base metals and the mass fraction of each metal in the mixture. Figure 3 presents the distribution of density in the model as a sample of material properties. The values of all material properties are presented in Table 1.

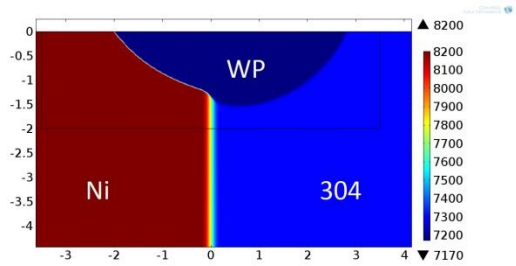


**Figure 3**. The distribution of density throughout the model

**Table 1:** Material Properties [13]

| Property | Ni | 304 | Solution |
|---|---|---|---|
| Solidus temperature (°C) | 1440 | 1400 | - |
| Liqudius temperature(°C) | 1460 | 1454 | - |
| Heat of fusion (kJ/kg) | 298 | 261 | - |
| Heat capacity (J/kg.K) | 617 | 720 | 780 |
| Density (kg/m$^3$) | 8200 | 7300 | 7230 |
| Thermal conductivity (W/m.K) | 80 | 33 | 40 |
| Viscosity (kg/m.s) | - | - | $6.3\times10^{-3}$ |
| Electric conductivity (S/m) | $1.4\times10^{-7}$ | $1.5\times10^{-6}$ | - |
| Temperature derivative of surface tension (N/m.K) | - | - | $-2\times10^{-4}$ |

## 4. Results and Discussion

The spot GTA welding of Ni to 304 stainless steel without consumable is simulated. The welding parameters are presented in Table 2. Following results have been obtained.

**Table 2.** The welding parameters used in the model

| | |
|---|---|
| Arc current | 150 A |
| Arc voltage | 14 V |
| Arc efficiency | 75 % |
| Welding time | 15 s |
| Sample size | 13×26×6.35 $mm^3$ |

Figure 4 shows the 3D weld pool profile after 15s of arc time in the sectioned sample along the x-axis. As expected the weld pool is not symmetric. The volume of molten material in the 304 side is larger due to lower melting temperature of 304 as compared to Ni.

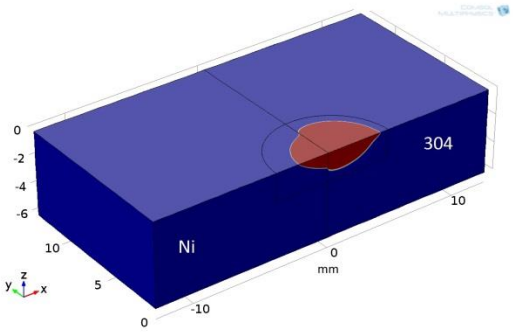


**Figure 4**. 3D weld pool profile

The velocity field and the weld profile in the xz-plane are presented in Figure 5. The maximum depth of penetration happens in the 304 side. Velocity field is shown by arrows and streamlines in the WP. Due to higher electrical conductivity of Ni, a higher Lorentz force is been created in the Ni side. This force pushes the fluid towards the 304 side. Maximum velocity happens at the surface in the 304 side and has a value of 0.147 m/s.

The top view (xy-plane) of the WP and the velocity field are shown in Figure 6. The velocity field at the surface is under the effect of Marangoni convection. As a result of negative temperature derivative of surface tension, all velocity vectors point towards the boundaries of the weld. The value of the surface tension at the interface of solid-liquid is much higher than that of the center of the weld; accordingly the fluid is pooled to the corners.

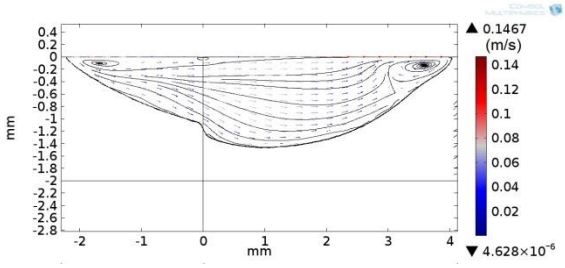


**Figure 5**. Velocity field in xz-plane

Deeper in the weld pool the effect of Marangoni convection diminishes and the fluid is driven by the Lorentz force. Figure 7 shows the velocity field at a surface parallel to xy-plane with *z=-0.5 mm*. As can be seen, the fluid moves from the Ni side towards the 304 side at the center of the weld and circulates back at the boundaries.

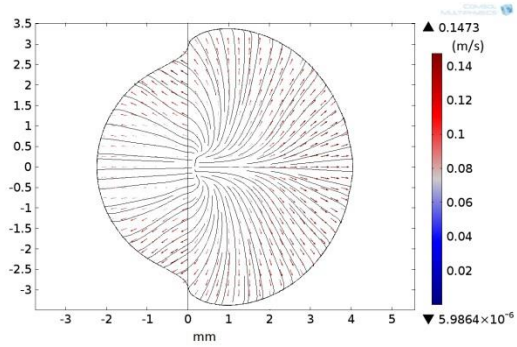


**Figure 6**. Velocity field in xy-plane

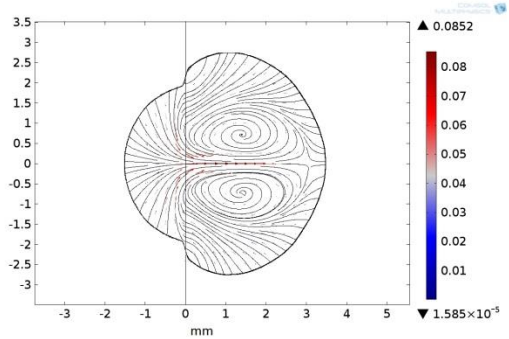


**Figure 7**. Velocity field in a surface parallel to xy-plane with z=-0.5 mm

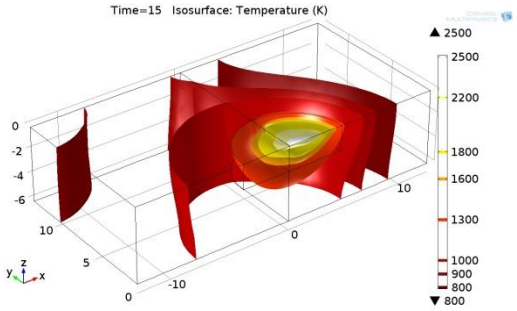


**Figure 8**. 3D isothermal surfaces

Figure 8 shows 3D temperature isotherms and Figure 9 shows the temperature distribution at the top surface of the weld (xy-plane). It is observed that the temperature distribution is highly asymmetric. The temperature at every point in the Ni side rises higher than that of the corresponding mirror point in the 304 side, due to lower thermal diffusivity of 304 stainless steel as compared to the thermal diffusivity of Ni.

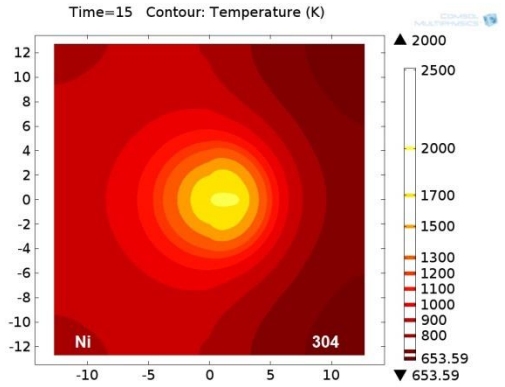


**Figure 9**. Temperature distribution at the top surface of the weld (xy-plane)

## 7. Conclusions

The GTA welding process of the dissimilar couple, Ni and 304 stainless steel, was simulated using finite element software COMSOL Multiphysics® 4.3b. The complicated interactions of different physical phenomena in the model perfectly were handled by COMSOL. Moreover the functions available in COMSOL are employed to take into account the changes in properties. The accomplishments of this study could be summarized in following items:

- The weld profile is asymmetric. The volume of the weld in the 304 steel side is larger than that in Ni side because the melting temperature of 304 is lower than that of Ni.
- Due to higher electric conductivity of Ni, Lorentz force is stronger in the Ni side; as a result the fluid is pushed from the Ni side towards the 304 side.
- The flow field at the top surface is driven by the Marangoni convection.
- The mean temperature in the Ni side is higher than that in the 304 side; however maximum temperature happens in the 304 side.

## 8. References


1. Kou, S., *Welding Metallurgy*, Wiley, New Jersey, pp. 97-121, (2003),
2. Bahrami, A., Aidun, D. K., Modeling of Transport Phenomena in Dissimilar Welding of 2205 Duplex Stainless Steel to 1018 Carbon Steel, *Trends in Welding Research 2012: Proceedings of the 9th International Conference (ASM International*), (2012)
3. Aidun, D. K. et al, "Effect of Convection on the Microstructure of Dissimilar Welds," *Proc. Int. Symposium of Computer- Aided Welding Engineering*, China, (2006)
4. Zacharia, T. *et al*, "Three-Dimensional Transient Model for Arc Welding," *Metallurgical Transactions B*, Vol. 20B (1989) , pp. 645-659.
5. Fan, H. G . *et al*, "Heat Transfer and Fluid Flow in a Partially or Fully Penetrated Weld Pool in Gas Tungsten Arc Welding," *Int.J Heat Mass Tras.* Vol. 44 (2001), pp. 417-428.
6. Tanaka, M. *et al*, "Prediction of Weld Pool Profile Using Plasma Physics," *J. Phys. D: Appl. Phys.*, Vol. 40, (2007), pp. R1-R23.
7. Lu, F. *et al*, " Modeling and Finite Element Analysis on GTAW arc and weld pool," *Computational Material Science*, Vol. 29 (2004), pp. 371-378.
8. Chakraborty, N. et al, "Modeling of Turbulent Molten Pool Convection in Laser Welding of Copper- Nickel Dissimilar Couple," *Int. J. Heat Mass Trans*. Vol.50 (2007), pp. 1805-1822.
9. Mukherjee, S. et al, "Transport Phenomena in Conduction Mode Laser Beam Welding

of Fe-Al Dissimilar Couple with Ta Diffusion Barrier," *Int. J. Heat Mass Trans.*, Vol. 53 (2010), pp. 5274-5282

10. Traidia, A. *et al*, "Optimal Parameters for Pulsed Gas Tungsten Arc Welding in Partially and Fully Penetrated Weld Pools," *Int. J. Thermal Science,* Vol. 49 (2010) pp. 1197-1208.
11. Zhang, W. *et al*, "Modeling of Heat Transfer and Fluid Flow during Gas Tungsten Arc Spot Welding of Low Carbon Steel," *Journal of Applied Physics,* Vol. 93, No. 5 (2003), pp.3022-3033.
12. Mills ,K. C. Recommended Values of Thermophysical Properties for Selected Commercial Alloys , *ASM International* (Cambridge, England, 2002).